Journal of King Saud University – Science 34 (2022) 101996

Contents lists available at ScienceDirect

Journal of King Saud University – Science

journal homepage: www.sciencedirect.com

Original article

Biosynthesized silica-based zinc oxide nanocomposites for the sequestration of heavy metal ions from aqueous solutions

Rishav Garg [a], Rajni Garg [b,*], Nnabuk Okon Eddy [c], Abdulaziz Ibrahim Almohana [d], Sattam Fahad Almojil [d], Mohammad Amir Khan [a], Seung Ho Hong [e]

[a] Department of Civil Engineering, Galgotias College of Engineering & Technology, Greater Noida, Uttar Pradesh 201310, India
[b] R&D Department, Institute of Sci-Tech Affairs, Mohali, Punjab 140301, India
[c] Department of Pure and Industrial Chemistry, University of Nigeria, Nsukka, Enugu State, Nigeria
[d] Department of Civil Engineering, College of Engineering, King Saud University, Riyadh 11421, Saudi Arabia
[e] Department of Civil & Environmental Engineering, Hanyang University ERICA Campus, Ansan 15588, South Korea

ARTICLE INFO

Article history:
Received 7 February 2022
Revised 15 March 2022
Accepted 22 March 2022
Available online 26 March 2022

Keywords:
Heavy metal ions
Water treatment
Adsorption
Nanocomposites
Chemisorption

ABSTRACT

In the present study, biosynthesized silica-based zinc oxide nanocomposites (nano-SZO) have been explored as nanoadsorbent for sequestrating heavy metal ions viz. Ni^{2+}, $Cd^{2+}$and Cu^{2+} from synthetic medium. The nanocomposites have been obtained by utilization of agricultural waste by means of green synthetic approach with an average particle size of 30.52 nm and a pH at zero-point charge as 4.8. The process has been optimized at a pH equal to 5.0 for Ni^{2+} and 6.0 for Cu^{2+} and Cd^{2+}. Adsorption was best described by Langmuir isotherm and the highest value of maximum adsorption capacity, q_m of nano-SZO was obtained for Cu^{2+} (32.53 mg/g), Ni^{2+} (32.10 mg/g), and Cd^{2+} (30.98 mg/g). The studied heavy metal ions are considerably adsorbed by the nano-SZO through chemisorption by active binding with polyhydroxy functionalities attached at the surface of the nanoadsorbent confirming the utilization of biosynthesized nano-SZO as eco-friendly and efficient nano adsorbents for the sequestration of heavy metal ions.

1. Introduction

Increasing industrialization and population growth worldwide have resulted in a rise in the concentration of polycyclic aromatic hydrocarbons, heavy metals, nutrients and other chemicals in air, water, and soil leading to severe issue of environmental pollution (Almomani et al., 2020). The major sources of heavy metals include industrial effluents released from mining (Khoso et al., 2021), electroplating, surface finishing (Jabasingh et al., 2018), and chemical production (Zhang et al., 2020) in addition to domestic and agricultural run-offs (Esfandiar et al., 2022). Being non-biodegradable and toxic, heavy metal ions get accumulated in the water resources causing adversative effects on aquatic animals as well as human beings (Garg et al., 2021). Accessibility to clean water for human consumption is the arousing concern with limitation of water resources arousing need for water treatment and remediation (Fan et al., 2021).

Adsorption has been considered most suitable with ease of operation, wide applicability, and cost-effectiveness (Almomani et al., 2020). Natural (Greathouse et al., 2015) and synthetic inorganic minerals (Borhade et al., 2015), Activated carbon (Bohli et al., 2017), natural (Huo et al., 2020) and functionalized polymers (Igberase et al., 2017) as well as biosorbents in the form of dried powder or ash obtained from leaves, peels (Garg et al., 2020), bark, husk and shells (Esfandiar et al., 2022) have been extensively used as adsorbents. With advent of nanotechnology and green chemistry, researchers have explored potential of green synthesized nanomaterials in solving environmental issues (Garg et al., 2021; Muhammad et al., 2021). Significant attempts have been done with utilization of nanomaterials as effective adsorbents for heavy metal ions (Khoso et al., 2021), dyes (Cheon et al., 2019), pharmaceuticals

* Corresponding author.
E-mail addresses: rishavgarg@science.org.in (R. Garg), rajnigarg@science.org.in (R. Garg), okon.nnabuk@unn.edu (N. Okon Eddy), aalmohanna@ksu.edu.sa (A. Ibrahim Almohana), salmojil@ksu.edu.sa (S. Fahad Almojil).

Peer review under responsibility of King Saud University.

Production and hosting by Elsevier

https://doi.org/10.1016/j.jksus.2022.101996
1018-3647/

and gases (Muhammad et al., 2021) as well with enhanced adsorption efficiency, ease of separation and regeneration.

Some of the nanomaterials that have been used as nano-adsorbents include zerovalent metal nanoparticles such as gold (Poornima et al., 2016), iron (Oprčkal et al., 2017), and silver (Cheon et al., 2019); metal oxide nanoparticles such as iron oxide (Jain et al., 2018), zinc oxide (Sharma et al., 2020) and calcium oxide (Jalu et al., 2021), carbon nanotubes and graphene (Nasrollahzadeh et al., 2021), mesoporous silica (Rovani et al., 2018), zeolites (Fan et al., 2021), and nanocomposites (Zhang et al., 2020). The hybrid nanoporous materials have also been explored as efficient nanoadsorbents (Muhammad et al., 2020; Muhammad and Mohanty, 2019).

Zinc oxide nanoparticles (ZnO NP) have exhibited significant potential in water treatment and remediation with their low toxicity, optical properties, band gap, photocatalytic potential and antibacterial action (Sharma et al., 2020). However, to the best of our knowledge, the work on green-synthesized silica-based zinc oxide composites, with valorization of agricultural waste, for use as nanoadsorbents has not been explored. With due consideration of unique characteristics of ZnO NP and extensive use of silica in adsorption, this paper reports the biosynthesis of silica supported ZnO nanocomposites (nano-SZO) from rice husk, an agricultural waste and a rich source of silica and various phytochemicals. The obtained nano-SZO were explored as nano-adsorbent for the sequestration of heavy metal ions viz. Ni^{2+}, $Cd^{2+}$and Cu^{2+} from synthetic wastewater.

2. Materials and methods

2.1. Materials

All the chemicals used in this study were of analytical grade and procured from Merck, Mumbai. Rice husk was obtained from a local agricultural field as an agricultural waste. The husk was cleaned by washing with tap water followed by dil. HCl and de-ionized water. It was dried out in the sunlight and powdered for further use.

2.2. Methods

Nano-SZO were fabricated by modification of the already reported method by (Sebastian et al., 2018). 25 g of powdered husk was boiled in presence of 2 M NaOH solution for 3 hrs at 353 K to obtain the extract. 0.1 M solution of zinc nitrate hexahydrate was treated with extract in a 1:1 ratio (after trial of varying molar ratios) with constant stirring using a magnetic stirrer at 353 K. The mixture was aged for 24 hrs., centrifuged and rinsed with de-ionized water before being dried in a hot air oven and stored for future usage as nano-adsorbents.

The surface morphological analysis of nano-SZO was performed by Scanning electron microscope (Model Jeol JSM-6100) and the attached functionalities were characterized by FTIR (Model Perkin Elmer Spectrum 400). The zeta potential of nano-SZO at pH from 1 to 7 was measured by Malvern zeta potential analyser (Model Zetasizer Nano ZS90). X-Ray diffraction (XRD Model PANalytical X'Pert Pro) was used to analyse the crystallinity of nano-SZO. A microprocessor-based pH-meter (Model 1010 Labtronics) was used to monitor the pH of the solutions. Atomic absorption spectrophotometer (Model PerkinElmer PinAAcle 900T) was used to monitor the residual ion concentration.

De-ionized water was used to formulate synthetic media (10 mg/L) of Cu^{2+}, Ni^{2+}, and Cd^{2+} and further diluted to obtain the desired concentration. Batch experiments were performed by adding a known amount of nano-SZO (0.10–0.60 g/L) to 100 mL of the solution containing a known amount of heavy metal ions (10–20 mg/L), with agitation at 298 K, for a contact period of 60 min. pH of the solution was varied (1.0–7.0) by adding the required amount of dil. HCl or dil. NaOH and the mixture was left for equilibration. Thermodynamic analysis was carried out at 288–328 K. The sludge was filtered and residual ion concentration was analysed. Fig. 1 shows the program for analysis of adsorption data. 0.1 M HCl was used for the regeneration of exhausted nano-SZO from the sludge.

3. Results and discussion

3.1. Characterization of nano-SZO

Fig. 2 shows XRD pattern for nano-SZO with sharp peaks representing crystalline nature of nano-SZO and micrographs having roughly spherical particles in a heterogenous matrix. The average size of nano-SZO was computed as 30.52 nm using the Scherrer equation (Fan et al., 2017). The pH at zero-point charge (pH_{pzc}) was estimated as 4.8. FTIR of nano-SZO (Fig. 2) shows characteristic peaks at 537.57 cm^{-1} (Zn-O stretching modes), 1127.36 and 1030.58 cm^{-1} (Si-O stretching modes) (Doermbach et al., 2014). The functionalities attached with nano-SZO were validated by characteristic band at 3321.68 cm^{-1} (O–H bending modes), medium peaks at 2941.66 cm^{-1} and 2835.41 cm^{-} (asymmetric methylene stretching modes), small peaks at 1719.86 cm^{-1} (C = O stretching modes) and other peaks at 1458.34 and 1409.31 cm^{-1} attributed to C—H bending modes (Bansal et al., 2022; Sarwar et al., 2021).

3.2. Batch adsorption studies

The equilibrium adsorption capacity, q_e of nano-SZO (0.1 g/L) for heavy metal ions (10 mg/L) q_e increased with increase in pH at 298 K to attain a maximum at pH = 5.0 for Ni^{2+} and 6.0 for Cu^{2+} and Cd^{2+} (Fig. 3a). This pH was considered as optimal pH for further adsorption studies. The polyhydroxy and carboxy functionalities get protonated at pH lower than pH_{pzc} with the abundance of H^{+} ions that compete and repel the positively charged metal ions leading to lesser adsorption. At pH higher than pH_{pzc}, the heavy metal ions get favourably adsorbed by the adsorbent due to increased electrostatic attractions with the negatively charged adsorbent surface (Fato et al., 2019).

The removal efficiency of an adsorbent is affected by its dosage as evident in Fig. 3b with a rapid increase with the increase in nano-SZO dosage from 0.1 to 0.4 g/L and then no significant increase was obtained with the dosage increase to 0.6 g/L. Thus 0.4 g/L of nano-SZO was considered as the optimum dose for use in the other studies. The removal efficiency of nano-SZO at a dosage of 0.4 g/L was obtained as 91.52% (Ni^{2+}), 93.89% (Cd^{2+}) and 96.91% (Cu^{2+}). The initial increase can be ascribed to the increase in the adsorptive sites with increase in dosage of nano-SZO while the later observation may be linked to the overcrowding of nano-SZO at higher dosage leading to overlapping of the active sites (Khoso et al., 2021).

The effect of contact duration was studied for 60 min. at the optimized pH for heavy metal ion solution (10 mg/L) at a nano-SZO dosage of 0.4 g/L at 298 K. The heavy metal ions diffuse towards the surface of nano-SZO and invade its porous matrix. The adsorbed quantity, q_t was found to increase till equilibrium was attained at specific time (20 min. for Ni^{2+} and 15 min. for Cu^{2+} and Cd^{2+}). The observation reflects differential adsorptive behaviour the three metal ions for attainment of equilibrium (Fig. 3c). After the equilibrium, the removal efficiency was found to decrease owing to the saturation of the constant number of

Batch adsorption $q_e = \frac{(C_i - C_e)}{m} \times V$ $\%R = \left(\frac{C_i - C_e}{C_i}\right) \times 100$	• C_i (mg/L) = Initial concentration of heavy metal ions • C_e (mg/L) = Equilibrium concentration of heavy metal ions • q_e (mg/g) = Equilibrium adsorption capacity • V (L) = Volume of the solution • m(g) = Mass of the nano-SZO • $\%R$ = Percentage removal of heavy metal ions
Langmuir adsorption isotherm $\left(\frac{C_e}{q_e}\right) = \left(\frac{C_e}{q_m}\right) + \left(\frac{1}{K_{ads} q_m}\right)$	• q_m (mg/g) = Maximum adsorption capacity • K_{ads} (mg/L) = Langmuir adsorption constant
Freundlich adsorption isotherm $\ln q_e = \left(\frac{1}{n}\right) \ln C_e + \ln K_F$	• K_F (L/g) = Freundlich adsorption constant • n = Measure of the extent of adsorption on adsorbent
Temkin adsorption isotherm $q_e = \frac{RT}{b} \ln K_T + \frac{RT}{b} \ln C_e$	• b (kJ/mol) = Temkin constant related to the heat of adsorption • K_T = Equilibrium binding constant (L g^{-1}) • R = Universal gas constant (8.314 J mol^{-1} K^{-1}) • T = Absolute temperature in Kelvin
Dubinin-Radushkevich adsorption isotherm $\ln q_e = \ln q_m - K_{DR} \varepsilon^2$	• K_{DR} (mol^2 kJ^{-2}) = Dubinin-Radushkevich constant • E_{DR} (kJ mol^{-1}) = Mean free energy of adsorption $\left(E_{DR} = \frac{1}{\sqrt{2K_{DR}}}\right)$ • ε (kJ mol^{-1}) = Polanyi potential $\left(\varepsilon = RT \ln\left(1 + \frac{1}{C_e}\right)\right)$

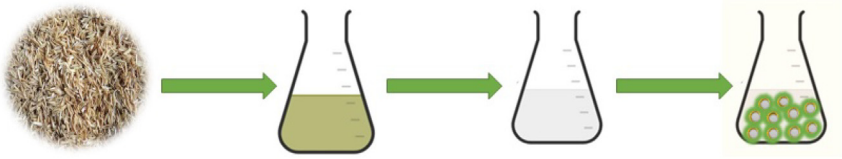

Pseudo-first-order model $\ln(q_e - q_t) = \ln q_e - k_1 t$	• q_t (mg/g) = Adsorption capacity of nano-SZO at time t (min.) • k_1 (min^{-1}) = Rate constant for pseudo-first order model
Pseudo-second-order model $\frac{t}{q_t} = \frac{1}{k_2 q_e^2} + \frac{1}{q_e} t$	• k_2 (g/mg min) = Rate constant for pseudo-second order model
Elovich model $q_t = \frac{1}{\beta} \ln(\alpha\beta) + \frac{1}{\beta} \ln t$	• α (mg/ g.min) = Initial adsorption rate • β (g/mg) = Desorption constant
Inter-particle diffusion $q_e = k_{id} \sqrt{t} + C$	• k_{id} (mg/ g $min^{1/2}$) = Rate constant for inter-particle diffusion • C (mg/g) = Model constant determining the boundary layer effect
Thermodynamic analysis $\ln K = \frac{\Delta S^o}{R} - \frac{\Delta H^o}{RT}$	• ΔS^o (J/mol K)= Standard entropy change • ΔH^o (kJ/mol)= Standard enthalpy change • ΔG^o (kJ/mol) = Standard Gibbs free energy change • K (L/mg)= Distribution coefficient

Fig. 1. Program for adsorption studies.

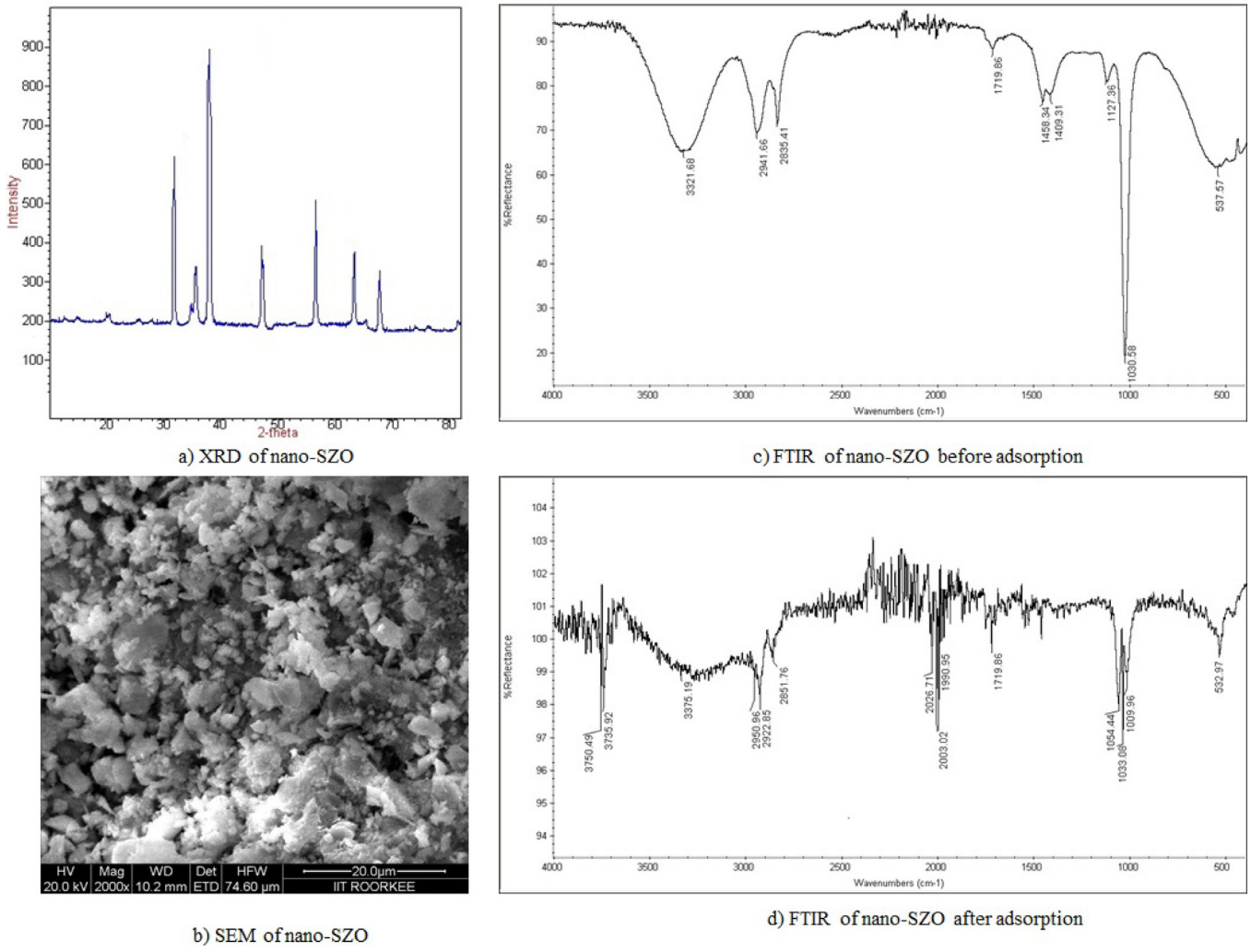

Fig. 2. Characterization of nano-SZO.

active sites in nano-SZO at equilibrium (Jain et al., 2018). The adsorption of heavy metal ions decreased with increase in initial concentration of heavy metal ion as evident in Fig. 3d. Higher energy sites are involved at low metal ion concentration and as the metal ion concentration increases, the saturation of higher energy sites induces the involvement of lower energy sites decreasing the adsorption efficiency (Bansal et al., 2022).

3.3. Adsorption isotherms

Fig. 4 illustrates the plots for the linear fits of the isotherms for the adsorption of heavy metal ions (10–20 g/L) at optimized pH onto nano-SZO (0.4 g/L) at 298 K and the values of the computed parameters are listed in Table 1.

The minimal deviation was obtained for the linear form of Langmuir isotherms (considering the monolayer coverage of the adsorbate on homogeneous surface of adsorbent) as indicated by the high value of regression coefficients, R^2 (0.9946–0.9979) for the fitted equation (Fig. 4a). The extent of adsorption increases with the increasing electronegativity of Cu^{2+} (1.9), Ni^{2+} (1.8), and Cd^{2+} (1.7) in Pauling scale resulting in increased affinity (Igberase et al., 2017). The values of the adsorption parameter K_{ads}, a measure of the extent of affinity of the adsorbent for the adsorbate were obtained in the order as Cu^{2+} (3.32 L/mg), Ni^{2+} (2.04 mg/g), and Cd^{2+} (1.81 mg/g).

Freundlich isotherm model considers the exponentiated distribution of active sites on a heterogeneous surface of adsorbent with the variance of the binding energies for multilayer adsorption. The intercept of the linear plot (Fig. 4b) was used to determine the value of Freundlich constant, K_F (22.43–25.26 mg/g) and the slope was used to determine the value of 1/n (<10) for all the studied systems indicating the favourability of the adsorption onto nano-SZO. The varying extent of adsorption can be linked to the differential affinity of functionalities linked at the active sites. Fig. 4c shows the plots for Temkin adsorption isotherm. The values of Temkin constant, b_T was obtained less than unity (0.73–0.79 kJ/mol), for all the studied systems, supporting physiosorption of metal ions onto nano-SZO (Jain et al., 2018). The value of R^2 (0.9079–0.9299) were lesser than that of Langmuir model. Dubinin-Radushkevich isotherms (Fig. 4d) were used to compute the values for mean free energy of adsorption,E_{DR}. The corresponding values (2.38–3.77 kJ/mol) were obtained below 8 kJ/mol in favour of physiosorption (Zhang et al., 2020). The fitted plots were obtained with very low values of R^2 (0.7184–0.7943). Considering the better suitability of the Langmuir model, the adsorption of Ni^{2+}, Cu^{2+} and Cd^{2+} onto nano-SZO may have proceeded by monolayer formation on to nano-SZO surface.

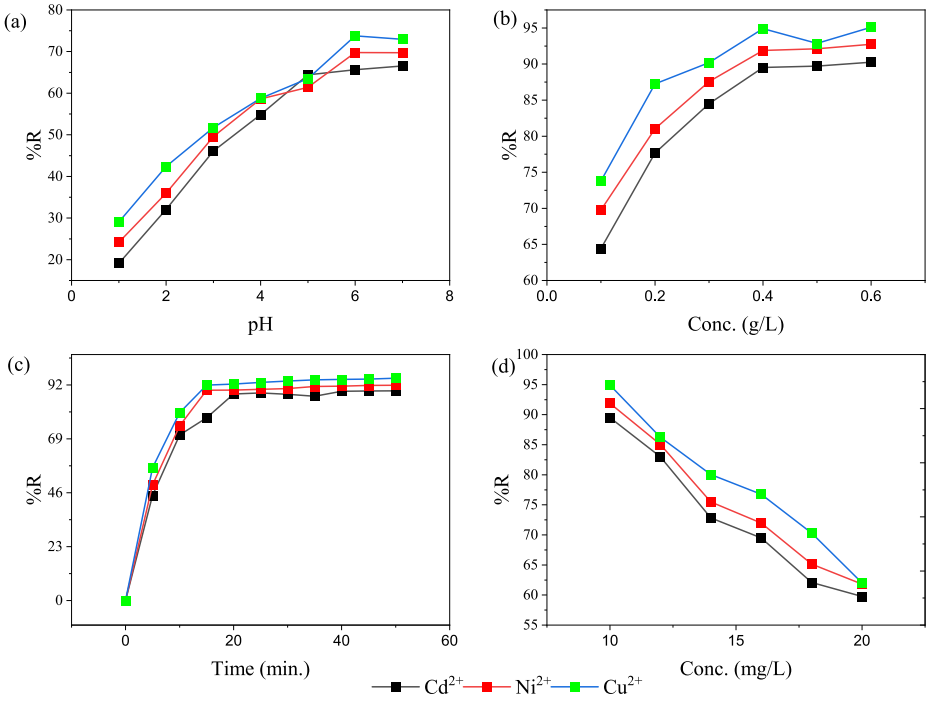

Fig. 3. Variation of removal efficiency of nano-SZO with (a) pH (b) adsorbent dosage (c) contact time period (d) concentration of heavy metal ions.

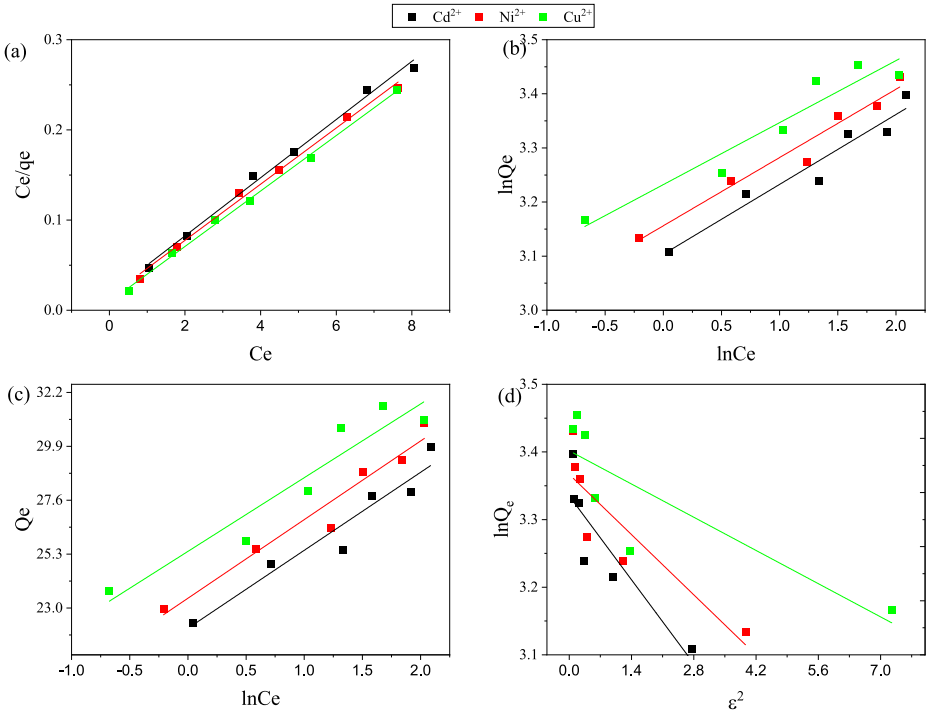

Fig. 4. (a) Langmuir isotherm (b) Freundlich isotherm (c) Temkin isotherm (d) Dubinin-Radushkevich isotherm plots for adsorption of metal ions on nano-SZO.

3.4. Adsorption kinetics

Fig. 5 illustrates the fitted plots for kinetic models with the values of the computed parameters for these models in Table 2. The values of R^2 (Table 4) were low (0.0.7491–0.7777) for the pseudo first-order model (Fig. 5a) and the experimental values of q_e didn't agree well with the computed values of q_e in case of Cu^{2+} and Cd^{2+}. The experimental data fitted well with pseudo second-order kinetics model with very high values of R^2 (0.9953–0.9979). The experimental values of q_e also agreed well with the computed values of q_e (Table 2). This model considers a direct relationship between the adsorption capacity of the adsorbent and the extent of occupied active sites on the adsorbent surface (Zhang et al., 2020). The fitted plots of Elovich and inter-particle diffusion models exhibited different behaviour with change in time indicating the role play of diffusion and adsorption (Jabasingh et al., 2018). The value of initial adsorption rate, α was computed from the intercept and slope was found very high in case of Cu^{2+} (73.08 mg/g min) followed by

Table 1
Isotherms constants for the adsorption of metal ions on nano-SZO.

Model Parameters	Cd^{2+}	Ni^{2+}	Cu^{2+}
Langmuir			
R^2	0.9946	0.9979	0.9975
K_{ads} (L/mg)	1.8066	2.0458	3.3175
q_m (mg/g)	30.9859	32.1054	32.5312
Freundlich			
R^2	0.9349	0.9588	0.9335
K_F (mg/g)	22.4327	23.5613	25.2657
n (L/mg)	8.439	8.4134	7.9367
Temkin			
R^2	*0.9299*	0.9524	0.9079
K_T (L/mg)	1.0302	1.0322	1.0328
b (kJ/mol)	0.7438	0.7379	0.7872
Dubinin-Radushkevich			
R^2	0.7943	0.7803	0.7184
q_m (mg/g)	28.0799	28.9884	30.0163
K_{DR} (mol^2/kJ^2)	0.0886	0.0636	0.0351
E_{DR} (kJ mol^{-1})	2.376	2.8037	3.7749

Table 2
Kinetics models parameters for adsorption of metal ions on nano-SZO.

Model parameters	Cd^{2+}	Ni^{2+}	Cu^{2+}
Experimental q_e (mg/g)	22.3798	22.9728	23.7276
Pseudo-first-order model			
R^2	0.7777	0.8204	0.7491
Q_e (mg/g)	9.0115	6.8958	6.1392
k_1 (min^{-1})	0.1324	0.1273	0.1144
Pseudo-second-order model			
R^2	0.9953	0.9959	0.9979
Q_e (mg/g)	23.6653	24.0161	24.5389
k_2 (g/mg min)	0.0163	0.0211	0.0257
Elovich model			
R^2	0.8371	0.7674	0.7767
α (mg/g min)	0.2247	0.2463	0.2766
β (g/mg)	19.0033	33.7930	73.0823
Inter-particle diffusion model			
R^2	0.7334	0.6534	0.6600
k_{id} (mg/g $min^{1/2}$)	2.1196	1.9149	1.7014
C(mg/g)	9.9541	11.8943	13.8151

Ni^{2+} (33.79 mg/g min), and Cd^{2+} (19.00 mg/g min). The sufficiently high values of the rate constant for inter-particle diffusion, k_{id} and the model constant C(mg/g) indicate the role of boundary layer effect (Zhang et al., 2020). However, very low values of R^2 for Elovich model and inter-particle diffusion model limits their suitability to describe the mechanism of the process. Thus, the adsorption of Ni^{2+}, Cu^{2+} and Cd^{2+} onto nano-SZO was considered to follow pseudo-second order kinetics. Further, nature of adsorption mechanism of was confirmed by thermodynamic studies.

3.5. Thermodynamic analysis

The removal efficiency of nano-SZO for Ni^{2+}, Cu^{2+} and Cd^{2+} was found to increase with increase in temperature reflecting the adsorption of Ni^{2+}, Cu^{2+} and Cd^{2+} onto nano-SZO as an endothermic process (Fig. 6a). The initial sharp increase till 298 K can be attributed to the increase in the mobility of the metal ions leading to faster diffusion and adsorption on the surface of nano-SZO (Jain et al., 2018). The removal efficiency exhibited a gradual increase from 298 to 328 K indicating the role of temperature in activation of the active sites. Standard enthalpy change, ΔH ° was computed from the slope and the standard entropy change, ΔS° was computed from the intercept of the linear plot of lnK against 1/T as shown in Fig. 6b. The values for standard free energy change, G along with other thermodynamic parameters have been given in supplementary information. The negative values of ΔH ° validate the adsorption as an endothermic process while the positive values of ΔS° indicate the increase of randomness at the surface of nano-SZO (Khoso et al., 2021). The negative values of G indicate the adsorption of Ni^{2+}, Cu^{2+} and Cd^{2+} onto nano-SZO as spontaneous.

3.6. Mechanism for adsorption

The adsorption of metal ions onto the surface of adsorbent have been considered a complex phenomenon governed by various fac-

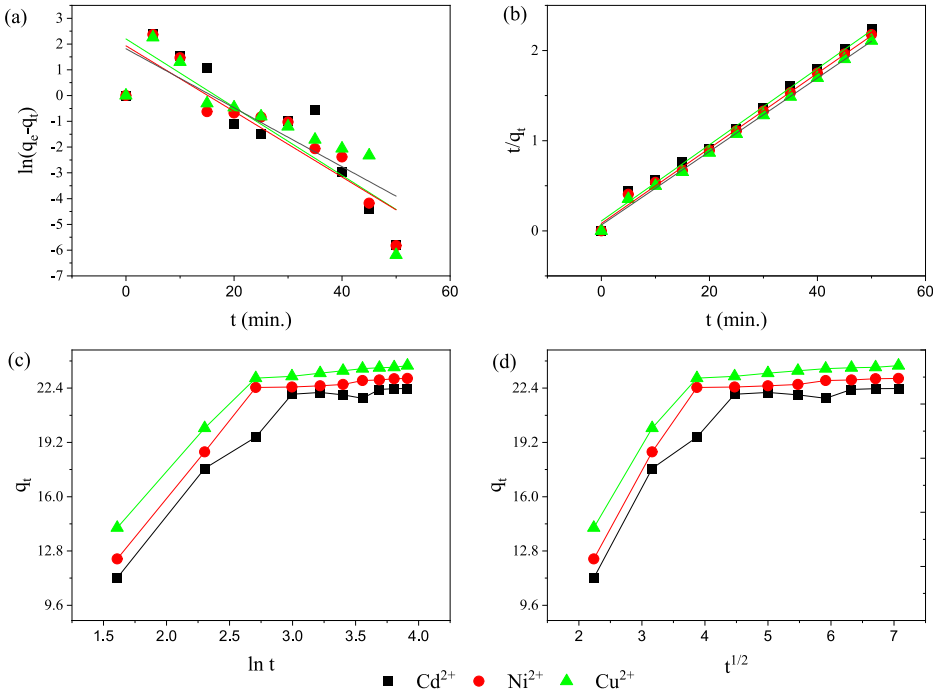

Fig. 5. (a) Pseudo-first order model (b) Pseudo-second order model (c) Elovich kinetic model (d) intra particle diffusion model plots for adsorption of metal ions on nano-SZO.

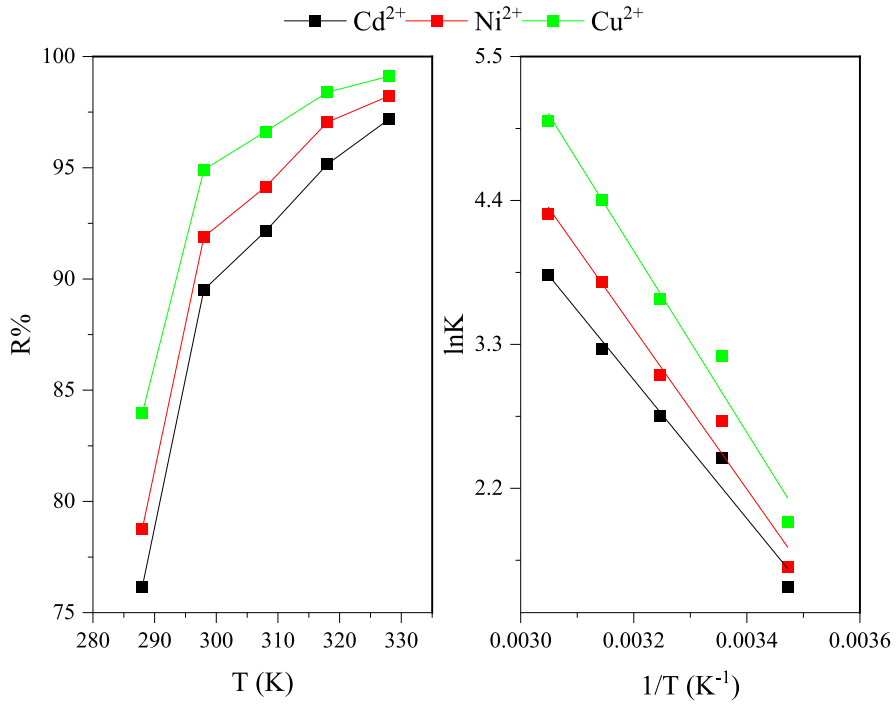

Fig. 6. Thermodynamics of nano-SZO(a) effect on removal efficiency with change in temperature (b) Van't Hoff plots for adsorption of metal ions on nano-SZO.

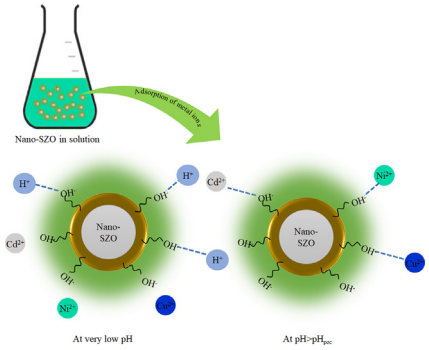

Fig. 7. Mechanism for adsorption of metal ions on nano-SZO.

tors. Researchers have reported influence of physico-chemical properties of the metal ions on their uptake (Fan et al., 2021). The role of electrostatic attractions between the positively charged metal ions and differently charged surface of the adsorbent depending upon the pH_{pzc} (Xin et al., 2012), complexation by formation of a chemical bond between the functionalities on the surface of the adsorbent and the metal ions (Igberase et al., 2017), and ion-exchange involving exchange of positively charged metal ions with some ions present on the surface of the adsorbent (Mobasherpour et al., 2012) etc. has been signified in the literature (Esfandiar et al., 2022). The adsorption kinetics, and adsorption isotherm analysis in this study reflect the formation of a monolayer on the surface of the nano-SZO. The endothermic process with sufficiently positive values of ΔH^o also indicate the role of chemisorption involving metal ions and the surface functionalities in the process. The shift in stretching vibrations of OH-groups and appearance of new peaks (Fig. 2) confirm the chemical interaction between the polyhydroxy and carboxyl functionalities attached on the surface of nano-SZO as illustrated in Fig. 7.

4. Conclusion

The adsorption of three heavy metal ions, Ni^{2+}, Cu^{2+} and Cd^{2+} onto nano-SZO has been studied. Nano-SZO was synthesized by green synthetic technique utilizing agricultural waste. The process parameters were optimized as pH = 5.0 for Ni^{2+} and 6.0 for Cu^{2+} and Cd^{2+} at 298 K and nano-SZO dosage of 0.4 g/L for a heavy metal ion concentration of 10 mg/L. Nano-SZO exhibited significant maximum adsorption capacities as obtained from Langmuir adsorption isotherm. The adsorption followed pseudo-second order kinetics with chemisorption as the adsorption route. The study confirmed the potential of biosynthesized nano-SZO as an efficient nano-adsorbent for sequestrating the studied heavy metal ions through an endothermic and spontaneous process.

Declaration of Competing Interest

The authors declare that they have no known competing financial interests or personal relationships that could have appeared to influence the work reported in this paper.

Acknowledgements

Funding: The authors would like to acknowledge the support provided by Researchers Supporting Project Number (RSP-2021/303), King Saud University, Riyadh, Saudi Arabia.

References

Almomani, F., Bhosale, R., Khraisheh, M., kumar, A., Almomani, T., 2020. Heavy metal ions removal from industrial wastewater using magnetic nanoparticles (MNP). Appl. Surf. Sci. 506, 144924. https://doi.org/10.1016/j.apsusc.2019.144924.

Bansal, M., Garg, R., Garg, V.K., Garg, R., Singh, D., 2022. Sequestration of heavy metal ions from multi-metal simulated wastewater systems using processed agricultural biomass. Chemosphere 296, 133966. https://doi.org/10.1016/j.chemosphere.2022.133966.

Bohli, T., Ouederni, A., Villaescusa, I., 2017. Simultaneous adsorption behavior of heavy metals onto microporous olive stones activated carbon: analysis of metal interactions. Euro-Mediterranean J. Environ. Integr. 2, 1–15. https://doi.org/10.1007/s41207-017-0030-0.

Borhade, A.V., Kshirsagar, T.A., Dholi, A.G., Agashe, J.A., 2015. Removal of heavy metals Cd2+, Pb2+, and Ni2+ from aqueous solutions using synthesized azide cancrinite, Na8[AlSiO4]6(N3)2.4(H2O)4.6. J. Chem. Eng. Data 60 (3), 586–593. https://doi.org/10.1021/je500698x.

Cheon, J.Y., Kim, S.J., Park, W.H., 2019. Facile interpretation of catalytic reaction between organic dye pollutants and silver nanoparticles with different shapes. J. Nanomater. 2019, 1–8. https://doi.org/10.1155/2019/3257892.

Doermbach, K., Agrawal, G., Servos, M., Schipmann, S., Thies, S., Klemradt, U., Pich, A., 2014. Silica-coating of hematite nanoparticles using reactive water-soluble polyalkoxysiloxanes. Part. Part. Syst. Charact. 31 (3), 365–373. https://doi.org/10.1002/ppsc.201300234.

Esfandiar, N., Suri, R., McKenzie, E.R., 2022. Competitive sorption of Cd, Cr, Cu, Ni, Pb and Zn from stormwater runoff by five low-cost sorbents; Effects of co-contaminants, humic acid, salinity and pH. J. Hazard. Mater. 423, 126938. https://doi.org/10.1016/j.jhazmat.2021.126938.

Fan, H.L., Zhou, S.F., Jiao, W.Z., Qi, G.S., Liu, Y.Z., 2017. Removal of heavy metal ions by magnetic chitosan nanoparticles prepared continuously via high-gravity reactive precipitation method. Carbohydr. Polym. 174, 1192–1200. https://doi.org/10.1016/j.carbpol.2017.07.050.

Fan, X., Liu, H., Anang, E., Ren, D., 2021. Effects of electronegativity and hydration energy on the selective adsorption of heavy metal ions by synthetic nax zeolite. Materials (Basel). 14 (15), 4066. https://doi.org/10.3390/ma14154066.

Fato, F.P., Li, D.-W., Zhao, L.-J., Qiu, K., Long, Y.-T., 2019. Simultaneous Removal of Multiple Heavy Metal Ions from River Water Using Ultrafine Mesoporous Magnetite Nanoparticles. ACS Omega 4 (4), 7543–7549. https://doi.org/10.1021/acsomega.9b0073110.1021/acsomega.9b00731.s001.

Garg, R., Garg, R., Thakur, A., Arif, S.M., 2020. Water remediation using biosorbent obtained from agricultural and fruit waste. Mater. Today Proc. 46, 6669–6672. https://doi.org/10.1016/j.matpr.2021.04.132.

Garg, R., Rani, P., Garg, R., Eddy, N.O., 2021. Study on potential applications and toxicity analysis of green synthesized nanoparticles. Turkish J. Chem. 1690–1706. https://doi.org/10.3906/kim-2106-59.

Greathouse, J.A., Geatches, D.l., Pike, D.Q., Greenwell, H.C., Johnston, C.T., Wilcox, J., Cygan, R.T., 2015. Methylene blue adsorption on the basal surfaces of kaolinite: Structure and thermodynamics from quantum and classical molecular simulation. Clays Clay Miner. 63 (3), 185–198. https://doi.org/10.1346/CCMN.2015.0630303.

Huo, Z., Zhao, S., Yi, J., Zhang, H., Li, J., 2020. Biomass-based cellulose functionalized by phosphonic acid with high selectivity and capacity for capturing U(VI) in aqueous solution. Appl. Sci. 10, 2–3. https://doi.org/10.3390/APP10165455.

Igberase, E., Osifo, P., Ofomaja, A., 2017. The Adsorption of Pb, Zn, Cu, Ni, and Cd by Modified Ligand in a Single Component Aqueous Solution: Equilibrium, Kinetic, Thermodynamic, and Desorption Studies. Int. J. Anal. Chem. 2017, 1–15. https://doi.org/10.1155/2017/6150209.

Jabasingh, S.A., Belachew, H., Yimam, A., 2018. Iron oxide induced bagasse nanoparticles for the sequestration of Cr6+ ions from tannery effluent using a modified batch reactor. J. Appl. Polym. Sci. 135 (36), 46683. https://doi.org/10.1002/app.46683.

Jain, M., Yadav, M., Kohout, T., Lahtinen, M., Garg, V.K., Sillanpää, M., 2018. Development of iron oxide/activated carbon nanoparticle composite for the removal of Cr(VI), Cu(II) and Cd(II) ions from aqueous solution. Water Resour. Ind. 20, 54–74. https://doi.org/10.1016/j.wri.2018.10.001.

Jalu, R.G., Chamada, T.A., Kasirajan, D.R., 2021. Calcium oxide nanoparticles synthesis from hen eggshells for removal of lead (Pb(II)) from aqueous solution. Environ. Challenges 4, 100193. https://doi.org/10.1016/j.envc.2021.100193.

Khoso, W.A., Haleem, N., Baig, M.A., Jamal, Y., 2021. Synthesis, characterization and heavy metal removal efficiency of nickel ferrite nanoparticles (NFN's). Sci. Rep. 11, 1–10. https://doi.org/10.1038/s41598-021-83363-1.

Mobasherpour, I., Salahi, E., Pazouki, M., 2012. Comparative of the removal of Pb 2+, Cd 2+ and Ni 2+ by nano crystallite hydroxyapatite from aqueous solutions: Adsorption isotherm study. Arab. J. Chem. 5 (4), 439–446. https://doi.org/10.1016/j.arabjc.2010.12.022.

Muhammad, R., Attia, N.F., Cho, S., Park, J., Jung, M., Chung, J., Oh, H., 2020. Exploitation of surface heterogeneity and textural properties in nanoporous carbon fabrics for efficient iodine capture. Thin Solid Films 706, 138049. https://doi.org/10.1016/j.tsf.2020.138049.

Muhammad, R., Kim, S., Park, J., Jung, M., Lee, M.E., Chung, J., Jang, H., Oh, H., 2021. Chemical affinity-assisted H2 isotope separation using Ca-rich onion-peel-derived nanoporous carbon composite. Mater. Chem. Front. 5 (22), 8018–8024. https://doi.org/10.1039/D1QM00894C.

Muhammad, R., Mohanty, P., 2019. Iodine sequestration using cyclophosphazene based inorganic-organic hybrid nanoporous materials: Role of surface functionality and pore size distribution. J. Mol. Liq. 283, 58–64. https://doi.org/10.1016/j.molliq.2019.03.053.

Nasrollahzadeh, M., Sajjadi, M., Iravani, S., Varma, R.S., 2021. Carbon-based sustainable nanomaterials for water treatment: State-of-art and future perspectives. Chemosphere 263, 128005. https://doi.org/10.1016/j.chemosphere.2020.128005.

Oprčkal, P., Mladenovič, A., Vidmar, J., Mauko Pranjić, A., Milačič, R., Ščančar, J., 2017. Critical evaluation of the use of different nanoscale zero-valent iron particles for the treatment of effluent water from a small biological wastewater treatment plant. Chem. Eng. J. 321, 20–30. https://doi.org/10.1016/j.cej.2017.03.104.

Poornima, V., Alexandar, V., Iswariya, S., Perumal, P.T., Uma, T.S., 2016. Gold nanoparticle-based nanosystems for the colorimetric detection of Hg2+ ion contamination in the environment. RSC Adv 6 (52), 46711–46722.

Rovani, S., Santos, J.J., Corio, P., Fungaro, D.A., 2018. Highly Pure Silica Nanoparticles with High Adsorption Capacity Obtained from Sugarcane Waste Ash. ACS Omega 3 (3), 2618–2627. https://doi.org/10.1021/acsomega.8b0009210.1021/acsomega.8b00092.s001.

Sarwar, A., Wang, J., Khan, M.S., Farooq, U., Riaz, N., Nazir, A., Mahmood, Q., Hashem, A., Al-Arjani, A.B.F., Alqarawi, A.A., Abd_allah E.F., 2021. Iron oxide (Fe3o4)-supported sio2 magnetic nanocomposites for efficient adsorption of fluoride from drinking water: Synthesis, characterization, and adsorption isotherm analysis. Water (Switzerland) 13, 1514. https://doi.org/10.3390/w13111514.

Sebastian, A., Nangia, A., Prasad, M.N.V., 2018. A green synthetic route to phenolics fabricated magnetite nanoparticles from coconut husk extract: Implications to treat metal contaminated water and heavy metal stress in Oryza sativa L. J. Clean. Prod. 174, 355–366. https://doi.org/10.1016/j.jclepro.2017.10.343.

Sharma, R., Garg, R., Kumari, A., 2020. A review on biogenic synthesis, applications and toxicity aspects of zinc oxide nanoparticles. EXCLI J. https://doi.org/10.17179/excli2020-2842.

Xin, X., Wei, Q., Yang, J., Yan, L., Feng, R., Chen, G., Du, B., Li, H., 2012. Highly efficient removal of heavy metal ions by amine-functionalized mesoporous Fe 3O 4 nanoparticles. Chem. Eng. J. 184, 132–140. https://doi.org/10.1016/j.cej.2012.01.016.

Zhang, W., An, Y., Li, S., Liu, Z., Chen, Z., Ren, Y., Wang, S., Zhang, X., Wang, X., 2020. Enhanced heavy metal removal from an aqueous environment using an eco-friendly and sustainable adsorbent. Sci. Rep. 10, 1–19. https://doi.org/10.1038/s41598-020-73570-7.